BIOCHEMISTRY
including biophysical chemistry & molecular biology

ARTICLE

pubs.acs.org/biochemistry

Monovalent Cation Size and DNA Conformational Stability

Earle Stellwagen, Joseph M. Muse,[†] and Nancy C. Stellwagen*

Department of Biochemistry, University of Iowa, Iowa City, Iowa 52242, United States

ABSTRACT: The effect of monovalent cations on the thermal stability of a small model DNA hairpin has been measured by capillary electrophoresis, using an oligomer with 16 thymine residues as an unstructured control. The melting temperature of the model hairpin increases approximately linearly with the logarithm of increasing cation concentration in solutions containing Na^+, K^+, Li^+, NH_4^+, $Tris^+$, tetramethylammonium (TMA^+), or tetraethylammonium (TEA^+) ions, is approximately independent of cation concentration in solutions containing tetrapropylammonium (TPA^+) ions, and decreases with the logarithm of increasing cation concentration in solutions containing tetrabutylammonium (TBA^+) ions. At constant cation concentration, the melting temperature of the DNA model hairpin decreases in the order $Li^+ \sim Na^+ \sim K^+ > NH_4^+ > TMA^+ > Tris^+ > TEA^+ > TPA^+ > TBA^+$. Isothermal studies indicate that the decrease in the hairpin melting temperature with increasing cation hydrophobicity is not due to saturable, site-specific binding of the cation to the random coil conformation, but to the concomitant increase in cation size with increasing hydrophobicity. Larger cations are less effective at shielding the charged phosphate residues in B-form DNA because they cannot approach the DNA backbone as closely as smaller cations. By contrast, larger cations are relatively more effective at shielding the phosphate charges in the random coil conformation, where the phosphate−phosphate distance more closely matches cation size. Hydrophobic interactions between alkylammonium ions interacting electrostatically with the phosphate residues in the coil may amplify the effect of cation size on DNA thermal stability.

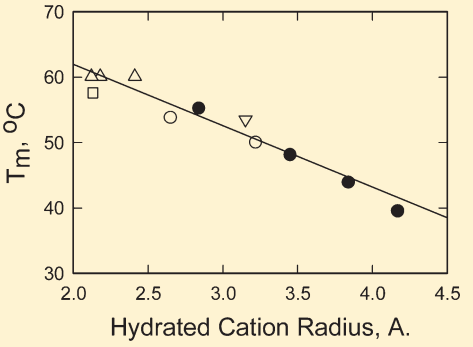

Monovalent cations are known to exhibit both stabilizing and destabilizing effects on the thermal stability of double-stranded DNA (dsDNA). Moderate concentrations of Na^+ and other alkali metal ions increase DNA stability with increasing cation concentration; however, salt concentrations in excess of 1 M cause the melting temperature to go through a maximum and then decrease.[1−6] Similar effects have been observed with small DNA hairpins.[7] The increase in the melting temperature with increasing cation concentration has been attributed to electrostatic shielding effects (e.g., refs 2, 8−11), counterion condensation,[12−14] and/or the effect of cations on water structure.[15,16] The maximum in the melting temperature and the subsequent decrease at still higher salt concentrations have been attributed to the effect of anions on DNA stability,[1] Hofmeister effects,[6] the decrease in the activity coefficient of Na^+ ions at high salt concentrations,[17] and/or the decrease in the activity coefficients of the nucleotide bases which are exposed to the solvent after denaturation.[18,19]

Alkylammonium ions also exhibit both stabilizing and destabilizing effects on DNA conformation. Moderate concentrations of tetramethylammonium (TMA^+) and tetraethylammonium (TEA^+) ions increase the stability of dsDNA with increasing cation concentration;[20−23] however, very high concentrations (≥2 M) cause the melting temperature to go through a maximum and then decrease.[20,22] Moderate concentrations of tetrapropylammonium (TPA^+) ions can either increase[23] or decrease[21] the melting temperature with increasing cation concentration. Tetrabutylammonium (TBA^+) and tetrapentylammonium ($TPeA^+$) ions decrease the melting temperature with increasing concentration.[21] Similar results have been observed with alkyltrimethylammonium (RMe_3N^+) and alkyltriethylammonium (REt_3N^+) ions.[22] The increase in the melting temperature with increasing alkylammonium ion concentration has been attributed to electrostatic shielding effects, as observed with the smaller cations.[20] The plateau and subsequent decrease in the melting temperature of duplex DNA observed for the smaller alkylammonium ions at high cation concentrations, and the decrease in the melting temperature observed with the larger alkylammonium ions at all cation concentrations, have been attributed to the hydrophobicity of the solvent[20,24] and/or to preferential binding of the alkylammonium ions to denatured, single-stranded DNA, pulling the equilibrium toward the random coil conformation.[21,23,25]

Because most of the studies cited above were carried out many years ago with polydisperse high molecular weight DNA samples, we have re-examined the effect of different organic and inorganic cations on DNA thermal stability, using a small well-characterized DNA hairpin with the sequence ATCCTATTTTTAGGAT (loop underlined) as our prototype DNA. NMR studies have shown that this oligomer forms a stable hairpin under a variety of ionic conditions and melts in a two-state helix−coil transition.[26,27] Using a hairpin instead of a duplex to measure DNA thermal stability simplifies the denaturation/renaturation equilibrium,

Received: September 24, 2010
Revised: February 25, 2011
Published: March 16, 2011

since the reaction is monomolecular in both the forward and reverse directions. An oligomer containing 16 thymine residues, called T16, was used as an unstructured random coil oligomer containing the same number of nucleotides.[28−31]

The thermal denaturation of the model hairpin has been measured by free solution capillary electrophoresis (CE). As described previously,[32,33] CE is a relatively straightforward method of analyzing the conformational transitions of small DNA oligomers because the free solution mobility depends only on the ratio between the effective charge of the oligomer and its frictional coefficient. When a DNA hairpin is denatured using either temperature or chemical reagents, the conformation becomes less compact, increasing the frictional coefficient while the effective charge remains approximately constant.[32,33] Hence, unless cations bind preferentially to one of the conformational isomers, the mobility of a hairpin will decrease upon denaturation until becoming equal to the mobility of a random coil containing the same number of nucleotides.[32,33] Gel electrophoresis has been used in a similar manner to monitor DNA thermal denaturation.[34] However, free solution capillary electrophoresis has the advantage that no gel matrix is required to separate small DNAs[35−37] and very small amounts of sample are required for each experiment.

In this study, the mobility of the model hairpin has been measured as a function of temperature in solutions containing different concentrations of Na^+, K^+, Li^+, NH_4^+, and $Tris^+$ ions as well as different concentrations of various alkylammonium ions. Isothermal CE measurements have been used to investigate the possible binding of NH_4^+ and TBA^+ ions to the model hairpin, using the previously described replacement ion method to monitor binding.[38] The results suggest that the effect of various alkylammonium ions on DNA thermal stability is not due to site-specific binding of the alkylammonium ions to the random coil conformation, pulling the equilibrium in that direction. Instead, cation size appears to be an important determinant of DNA thermal stability because cation size affects the relative electrostatic shielding of the phosphate residues in the hairpin and random coil conformations. Hydrophobic interactions between large alkylammonium ions condensed on the surface of DNA random coils may amplify the effect of cation size on the thermal stability of B-form DNA.

MATERIALS AND METHODS

DNA Samples. All DNA oligomers were synthesized by Integrated DNA Technologies (Coralville, IA), purified by polyacrylamide gel electrophoresis and characterized by mass spectrometry. Two hairpins were used in this work: the model hairpin with the sequence 5′-ATCCTATTTTTAGGAT (loop underlined) and a hairpin with an all G/C stem, called the reference hairpin, with the sequence 5′-GCCCGGTTTTCC GGGC (loop underlined). An oligomer containing 16 thymine residues (called T16) was used as an unstructured random coil control. Each oligomer was dissolved at a concentration of 1 μg/μL in 10 mM Tris-Cl buffer, pH. 8.0, and stored at −20 °C until needed. Aliquots of the model hairpin, reference hairpin, and T16 stock solutions were combined, diluted 10-fold with deionized water, and co-injected into the capillary for the melting studies.

Buffers. The background electrolytes (BGEs) used for all experiments contained diethylmalonate (DM) as the buffering anion. Stock solutions containing 0.67 M diethylmalonic acid [$(CH_3CH_2)_2C(COOH)_2$, Sigma-Aldrich, St. Louis, MO] were titrated to pH 7.3, the pK_a of the second carboxyl group, with a concentrated solution of Tris base (Research Products International Corp., Mt. Prospect, IL) or the hydroxide of one of the cations of interest (Sigma-Aldrich). Because the second carboxyl group of diethylmalonate is half-ionized at pH 7.3, the concentration of the cation in the stock solution was 1.0 M; the ionic strength was 1.34 M. Since the buffering ion is an anion, the cation in the BGE may be changed at will without altering the pH or buffering capacity of the solution. Control experiments have shown that the mobilities observed in solutions containing Tris-DM buffers are equal within experimental error to the mobilities observed in Tris-acetate buffers of the same ionic strength,[36] indicating that the mobility differences observed in different buffers are determined primarily by the cation in the BGE.

Capillary Electrophoresis. Capillary zone electrophoresis measurements were carried out with a Beckman Coulter (Fullerton, CA) P/ACE system MDQ capillary electrophoresis system run in the reverse polarity mode (anode on the detector side) with UV detection at 254 nm, as described previously.[38] LPA capillaries coated internally with linear polyacrylamide (Polymicro Technologies, Phoenix, AZ) were used to minimize the electroosmotic flow (EOF) of the solvent. Previous studies have shown that internal polyacrylamide coatings do not affect the observed mobility.[35] The capillaries were 30.9 ± 0.2 cm in length (20.6 ± 0.2 cm to the detector) and 75 μm in internal diameter, mounted in a thermostated liquid-cooled cassette. The applied electric field varied from ∼30 V/cm (the minimum available on the instrument) to ∼200 V/cm, depending on the conductivity of the BGE. Lower voltages were used with the more highly conductive solvents to keep the current less than ∼60 μA; under such conditions, Joule heating effects are negligible.[35] The DNA samples were injected hydrodynamically at low pressure (0.5 psi, 0.0035 MPa) for 3 s. The injection volume was ∼22 nL; the sample plug occupied ∼2.6% of the total capillary length. Control experiments have shown that the mobilities measured under these conditions are independent of DNA concentration, the length of the sample plug, and the applied electric field strength.[35]

The free solution mobility of an analyte such as DNA is determined by the ratio between its effective charge, Q, and its frictional coefficient, f (review: ref 39). If the residual EOF in the capillary is negligible in comparison with the mobility of the analyte, as is the case for the studies described here, the mobility, μ, can be calculated directly from the observed migration times using eq 1:

$$\mu = Q/f = L_d/Et \quad (1)$$

where L_d is the distance from the capillary inlet to the detector (in cm), E is the electric field strength (in V/cm), and t is the time required for the sample to migrate from the inlet to the detector (in seconds). The average standard deviation of mobilities measured for the same sample on any given day was ±0.2%; the day-to-day variation of the mobilities was ±1.6%. Such small mobility differences are within the sizes of the symbols in the mobility plots below. For convenience, the mobilities are reported in mobility units, m.u. (1 m.u. = 1×10^{-4} cm^2/(V s)).

Thermal Melting Studies. Thermal melting studies were carried out by measuring the mobility of the model hairpin, reference hairpin, and T16, co-injected into the capillary at the same time, at temperatures between 15 and 60 °C, the range available on the CE instrument. The capillary was allowed to equilibrate for at least 3 min at each temperature before the voltage was applied. Previous studies have shown a 3 min wait time is adequate for temperature equilibration.[32,33] The fractional

concentration of the model hairpin present at any temperature was calculated as described below. Plots of the fractional hairpin concentration vs temperature, called melting curves for brevity, were analyzed with a three-parameter Hill equation, using SigmaPlot. All melting curves were assumed to represent two-state conformational transitions.[27]

Binding Experiments. The possible binding of NH_4^+ and TBA^+ ions to the model hairpin and/or T16 was investigated by the replacement ion method.[38] In this method, a cation (such as Na^+) in the BGE is gradually replaced by another cation (such as NH_4^+ or TBA^+), keeping the total cation concentration constant. If neither Na^+ nor the replacement ion binds to the DNA in a site-specific manner, the mobility will change linearly with NH_4^+ or TBA^+ concentration due to differences in the intrinsic conductivities and viscosity B coefficients of the two ions. If the original cation and the replacement ion bind to the DNA with equal affinities, the mobility will also change linearly with replacement ion concentration. However, if one of the cations binds more strongly to the DNA than the other, the mobility will change nonlinearly with increasing replacement ion concentration. The curved mobility plots can then be fit by standard binding equations to calculate apparent dissociation constants. The apparent K_Ds obtained for the adenosine nucleotides by the replacement ion method agree with other values in the literature.[38] The binding of different monovalent cations to a 26-bp DNA duplex has also been determined by this method.[38]

RESULTS AND DISCUSSION

Hairpin Melting Occurs in the Fast Exchange Regime. A typical electropherogram observed for a solution containing the reference hairpin, model hairpin, and T16 (from left to right) in a background electrolyte (BGE) containing 300 mM TBA^+ is illustrated in Figure 1A. All three peaks are sharp and nearly Gaussian in shape, even though the measurements were made at 40 °C, close to the midpoint of the thermal transition in this BGE (see Figure 4A). The narrow peak observed for the model hairpin (middle peak) at this temperature indicates that the hairpin and coil conformations are in fast exchange in the transition region. Under such conditions, the observed mobility is the weighted sum of the mobilities of the two conformers.[32,33]

Thermal Dependence of the Mobility of T16. The mobilities observed for the reference hairpin, the model hairpin, and T16 in a BGE containing 300 mM TBA^+ are plotted as a function of temperature in Figure 1B. The mobility of T16, the open circles, increases linearly with increasing temperature, as expected for an oligomer that does not undergo a thermal transition within the investigated temperature range.[33] The increase in mobility of T16 with increasing temperature is due to the dependence of the viscosity, dielectric constant, and surface tension of water on temperature.[40−43] The mobility at any given temperature, T, can be predicted from the observed mobility at another temperature, e.g., 20 °C, using eq 2:

$$\mu_T = \mu_{20}\varepsilon_{rel}\gamma_{rel}/\eta_{rel} \quad (2)$$

Here, ε_{rel}, γ_{rel}, and η_{rel} are the ratios of the dielectric constant, surface tension, and viscosity of water, respectively, at 20 °C and at temperature T. The viscosity and dielectric constant corrections to the mobility have been discussed previously;[32,37] the surface tension correction takes into account nonpolar interactions between the analyte and the solvent[44−47] and the effect of different ions on the hydrogen-bonded structure of water.[48,49] The

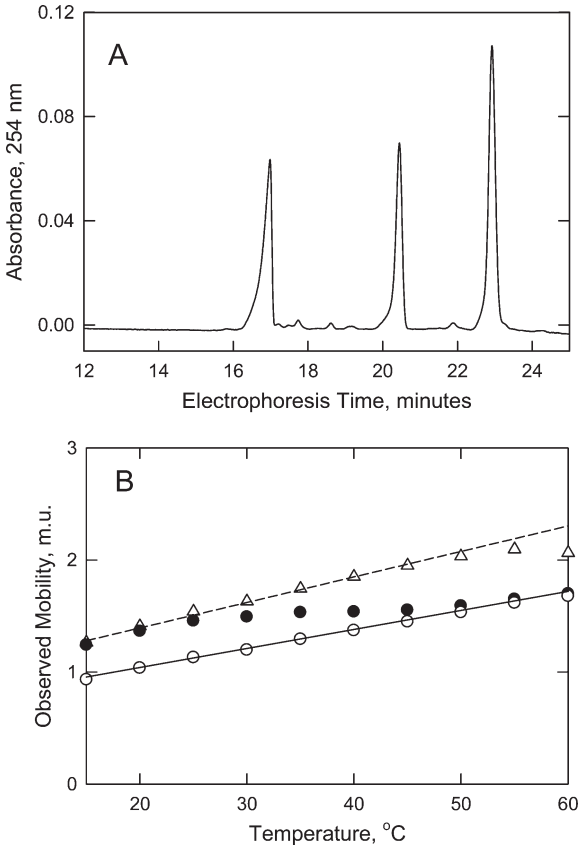

Figure 1. (A) Electropherogram observed for stable hairpin, model hairpin, and T16 (left to right) in a BGE containing 300 mM TBA^+ at 40 °C. The absorbance at 254 nm is plotted as a function of electrophoresis time. (B) Dependence of the mobility observed for the reference hairpin (△), the model hairpin (●), and T16 (○) on temperature in 300 mM TBA^+. The uncertainties in duplicate measurements of the mobility in this and subsequent figures are smaller than the sizes of the symbols. The solid and dashed lines were calculated using eq 2.

temperature dependence of the mobility of T16 predicted by eq 2, called the coil baseline, is indicated by the solid line in Figure 1B. The observed and predicted mobilities are equal, indicating that T16 has the conformation of an unstructured random coil in solution, as observed by others.[28−31] Since T16 does not undergo a thermal transition in the investigated temperature range, the mobility of an unstructured random coil at any temperature can be predicted using eq 2.

Thermal Dependence of the Mobilities of the Reference Hairpin and Model Hairpin. The thermal dependence of the mobility of the reference hairpin, which contains an all G-C stem, is indicated by the open triangles in Figure 1B. The thermal dependence predicted for the reference hairpin by eq 2 is indicated by the dashed line, termed the hairpin baseline. The hairpin baseline agrees with the mobilities observed for the reference hairpin at temperatures below 45 °C. Above this temperature, the mobility of the reference hairpin is lower than that predicted by the hairpin baseline, indicating the onset of the thermal denaturation of the reference hairpin.

The mobility of the model hairpin (filled circles in Figure 1B) is coincident with that of the reference hairpin at 15 °C, indicating that the model hairpin is primarily in the hairpin conformation at this temperature. As the temperature is increased, the

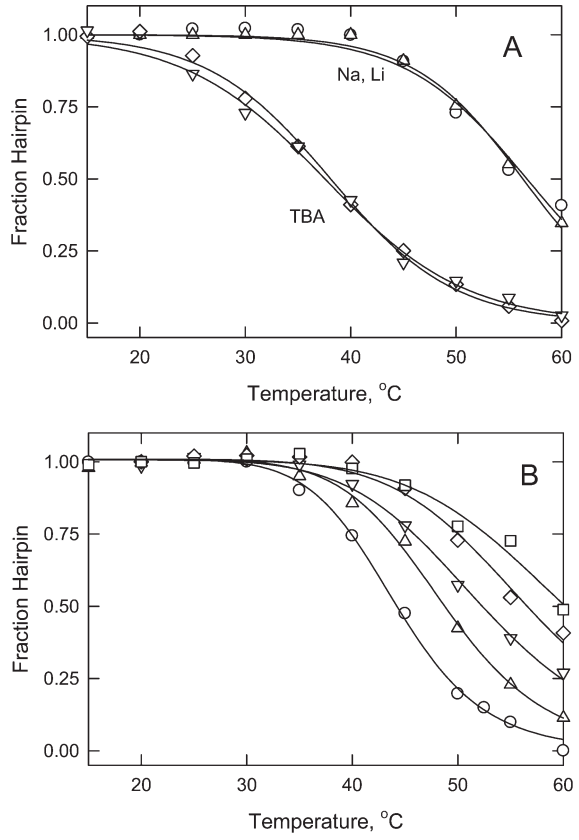

Figure 2. Melting curves observed for the model hairpin; the fractional hairpin population calculated from eq 3 is plotted as a function of temperature. (A) Melting curves observed in BGEs containing 100 mM: (○) Na^+; (△) Li^+; (◇, ▽) TBA^+ (replicate measurements). The curved lines correspond to fits of each melting curve to a three-parameter Hill equation. (B) Melting curves observed in BGEs containing various concentrations of Na^+ ions: (○) 10, (△) 25, (▽) 50, (◇) 100, and (□) 200 mM. The curved lines were drawn from a fit of the mobilities observed at all $[Na^+]$ to a three-parameter Hill equation.

mobility of the model hairpin becomes progressively lower than the hairpin baseline, becoming equal to the mobility of T16 at 60 °C. Hence, the conformational ensemble of the model hairpin in 300 mM TBA^+ gradually changes from essentially all hairpin to essentially all random coil as the temperature increases from 15° to 60 °C.

Melting Curves. The observed mobility of the model hairpin (filled circles in Figure 2A) and the hairpin and coil baselines (dashed and solid lines, respectively) can be used to calculate the fractional hairpin population, F_{hp}, at any temperature, T, using eq 3:[50]

$$F_{hp} = [(\mu_{\text{observed hairpin}} - \mu_{\text{coil baseline}})/ (\mu_{\text{hairpin baseline}} - \mu_{\text{coil baseline}})]_T \quad (3)$$

Representative plots of the thermal dependence of the fractional hairpin populations observed in BGEs containing 100 mM Na^+, Li^+, or TBA^+ are illustrated in Figure 2A. Each thermal dependence was fit with a three-parameter Hill equation, assuming a two-state helix−coil transition. The fitted curves are called melting curves, for brevity. The analysis provides the temperature at the midpoint of the transition, called the melting temperature, the standard error of the transition midpoint and the cooperativity of the transition.

The melting temperatures calculated from independent fits of the two melting curves measured in 100 TBA^+ were 38.1 and 37.6 °C. The average melting temperature, 37.8 ± 0.2 °C, is well within the estimated uncertainties of the fits, 0.6 and 0.8 °C, respectively. Similar results were observed in BGEs containing 100 mM Na^+ and 100 mM Li^+, where the melting temperatures were found to be 56.7 and 56.3 °C, respectively. The average melting temperature, 56.5 ± 0.2 °C, is also well within the standard errors of the fits, 0.7 and 0.3 °C, respectively. Hence, the standard errors obtained from the fits of the melting curves to a three-parameter Hill equation are a reasonable indication of the reproducibility of the measurements. The average standard error in the melting temperatures observed for the 49 different melting curves measured in this study was 0.4 °C.

Cooperativity of the Melting Transition. The cooperativity of the melting transitions observed in solutions containing 100 mM Na^+, Li^+, or TBA^+ can be determined from the melting curves in Figure 2A. The calculated cooperativity parameters are −5.4 ± 0.3 for Na^+ and Li^+ and −6.2 ± 0.4 for TBA^+. Hence, the cooperativity of the melting transition is essentially independent of the type of cation in the solution. The results agree with those of Collins and Rogers,[21] who measured the thermal melting of sonicated calf thymus and salmon egg DNAs by UV absorption spectroscopy. They found that the cooperativity of the thermal transition was independent of whether the solution contained NH_4^+ ions or one of the tetraalkylammonium ions.

By contrast, Melchior and von Hippel,[20] who studied the thermal denaturation of high molecular weight DNAs by UV absorption, found that the thermal transitions observed in 3.3 M TMA^+ or 2.4 M TEA^+ were sharper than those observed in 0.02 M Na^+ and attributed the increased cooperativity to a decrease in the thermal stability of G-C base pairs in concentrated tetraalkylammonium ion solutions. However, Melchior and van Hippel also observed that the differential stabilization of A-T and G-C base pairs was relatively small in solutions containing less than ~0.5 M TMA^+ or TEA^+, the concentration range used by us and by Collins and Rogers.[21]

Melting Curves Observed in Solutions Containing Different Concentrations of Na^+ Ions. Representative plots of the fractional hairpin population as a function of temperature and Na^+ ion concentration are illustrated in Figure 2B. The mobilities observed at temperatures below 35 °C were always coincident with the hairpin baseline. However, the observed mobilities did not reach the coil baseline at 60 °C, the highest temperature available on the CE instrument. Nonetheless, the fractional hairpin population can be calculated with confidence because the coil baseline at high temperatures can be predicted from the mobility of T16 and eq 2.

The good fits of the melting curves in Figure 2B to the measured data strongly suggest that the thermal denaturation of the model hairpin occurs as a two-state transition. Previous studies of the same model hairpin, using NMR chemical shift profiles to monitor the thermal denaturation of each base pair, found that each transition was well fitted by a two-state conformational equilibrium; the average melting temperature of all base pairs was 48 °C in solutions containing 15 mM Na^+ ions.[27] A gradual fraying of the terminal A-T base pair in the hairpin stem with increasing temperature was also observed, although some of the terminal base pairs remained intact up to the midpoint of the thermal transition. Fraying of some of the terminal base pairs

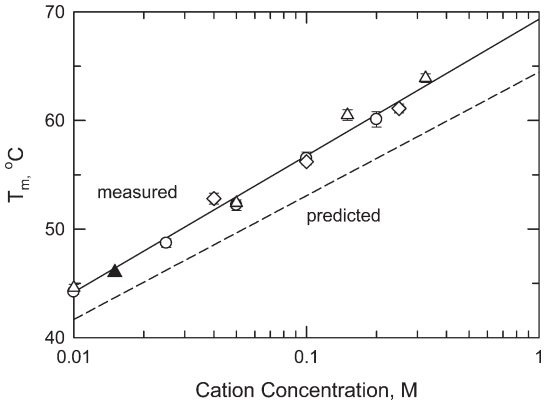

Figure 3. Dependence of the melting temperature, T_m, observed for the model hairpin on the logarithm of cation concentration in solutions containing the alkali metal ions: (○) Na^+; (◇) Li^+; or (△) K^+. In this and subsequence figures, error bars are indicated if the uncertainty in the melting temperature is larger than the size of the symbol. The solid triangle (▲) corresponds to the average T_m determined for the model hairpin in solutions containing 0.15 M Na^+, using UV absorption and NMR measurements.[27] The dashed line corresponds to the melting temperature predicted for the model hairpin by mfold.[58,59]

would not have had a significant effect on the electrophoretic mobility observed for the hairpin in the transition region, since the helix and coil conformations were in fast exchange and the observed mobility corresponds to the weighted average of the mobilities of the two conformers. Therefore, CE melting curves can accurately monitor the transition from a fully helical hairpin to a completely melted random coil.

Comparison of Melting Curves Observed in Solutions Containing Various Alkali Metal Ions. The melting temperatures observed for the model hairpin in solutions containing various [Na^+] ranged from 44.3 °C in 10 mM Na^+ (open circles in Figure 2B) to 60.1 °C in 200 mM Na^+ (open squares). Similar families of melting curves were obtained in BGEs containing Li^+ or K^+ ions (not shown). The melting temperatures observed in BGEs containing each of the three alkali metal ions are plotted in Figure 3 as a function of the logarithm of cation concentration. The melting temperature increased linearly with the logarithm of cation concentration over the range examined, as expected theoretically[40] and observed experimentally for duplex DNAs[2−4] and for DNA hairpins.[5,51−54] In addition, the melting temperatures were independent of the type of alkali metal ion in the BGE, in agreement with previous results.[55−57]

The melting temperatures measured for the model hairpin by UV absorption spectroscopy and by NMR in solutions containing 15 mM Na^+ ions were 44 and 48 °C, respectively.[27] The solid triangle in Figure 3 corresponds to 46 °C, the average of these two values. Since the average melting temperature falls on the straight line describing the melting temperatures measured by CE in BGEs containing 10−300 mM alkali metal ions, the melting temperatures measured by CE are in good agreement with the values obtained by other methods.

The melting temperatures measured by CE are also in reasonable agreement with the values predicted by the well-known structure-prediction program mfold,[58,59] as shown as the dashed line in Figure 3. Mfold predicts that only one hairpin structure is significantly populated during the melting transition. The predicted melting temperatures are ∼3 °C lower than those observed experimentally, within the estimated accuracy of the algorithm. The slopes of the lines describing the dependence of the predicted and observed melting temperatures on cation concentration are essentially parallel, again suggesting that the model hairpin melts in a two-state transition.

The slopes of the lines in Figure 3, $dT_m/d(\log [M^+])$, can be used to estimate the number of cations released per phosphate upon denaturation of the model hairpin.[14,32,60,61] Cation release is thought to occur because B-form DNA has a higher linear charge density than single-stranded DNA, causing greater numbers of cations to be condensed around the duplex (or hairpin) to shield the negatively charged phosphate residues.[12−14,40] The condensed ions are not site-bound to the DNA, but are fully hydrated and electrostatically trapped by the electric field of the closely spaced phosphate residues.[9,10,62−69] The number of cations released per phosphate upon denaturation, $\triangle n$, can be estimated using eq 4:[14,32,52,60,61]

$$\text{slope} = dT_m/d\log[M^+] = -2.3(\alpha R T_m^{\,2}/\triangle H^\circ)\triangle n \quad (4)$$

where [M^+] is the cation concentration, R is the gas constant, α is a factor that accounts for changes in the activity coefficient of the cation with concentration and is often set equal to 0.9,[52] and $\triangle H^\circ$ is the enthalpy of melting per nucleotide.[14,52,53,61] The factor in parentheses on the right-hand side of eq 4 is not significantly salt- and temperature-dependent and is often given the value of 50.[32,60,61] The slope of the solid line corresponding to the experimental melting temperatures corresponds to the release of 0.11 cations per phosphate upon denaturation of the model hairpin. This value is within the range of values observed for other small DNA hairpins in solutions containing Na^+ ions.[5,13,52−54,61] The slope of the dashed line calculated from the mfold algorithm corresponds to the release of 0.10 cations per phosphate upon hairpin denaturation, in good agreement with the experimentally determined value.

Melting Curves Observed in Solutions Containing Organic Cations. Typical melting curves observed for the model hairpin in solutions containing 200 mM NH_4^+, TMA^+, TEA^+, TPA^+, or TBA^+ are illustrated in Figure 4A. The melting curves are displaced to lower temperatures as the length of the hydrocarbon chain increases, indicating that the larger tetraalkylammonium ions are more effective destabilizers of hairpin structure. Similar melting curves were observed in BGEs containing 200 mM monopropylammonium (MPA^+), dipropylammonium (DPA^+), tripropylammonium ($TriPA^+$), and tetrapropylammonium (TPA^+) ions, as shown in Figure 4B. The melting curves are displaced to lower temperatures as the number of propyl side chains increases, indicating that the more highly substituted alkylammonium ions are more effective structure destabilizers.

The melting temperatures observed for the model hairpin in solutions containing NH_4^+, $Tris^+$ (tris[hydroxymethyl]aminomethane), or one of the tetraalkylammonium ions are plotted as a function of the logarithm of cation concentration in Figure 5A. In all cases, the melting temperatures exhibit a linear dependence on the logarithm of cation concentration over the range examined. At a given cation concentration, the melting temperatures decrease in the order $NH_4^+ > TMA^+ > Tris^+ > TEA^+ > TPA^+ > TBA^+$. It should also be noted that the slopes of the lines, $dT_m/d(\log [M^+])$, change from positive to negative as the size and hydrophobicity of the cation increases.

The slopes of the lines in Figure 5A suggest that ∼0.09 NH_4^+ ions are released per phosphate upon denaturation of the model hairpin and ∼0.04 cations are released per phosphate in BGEs

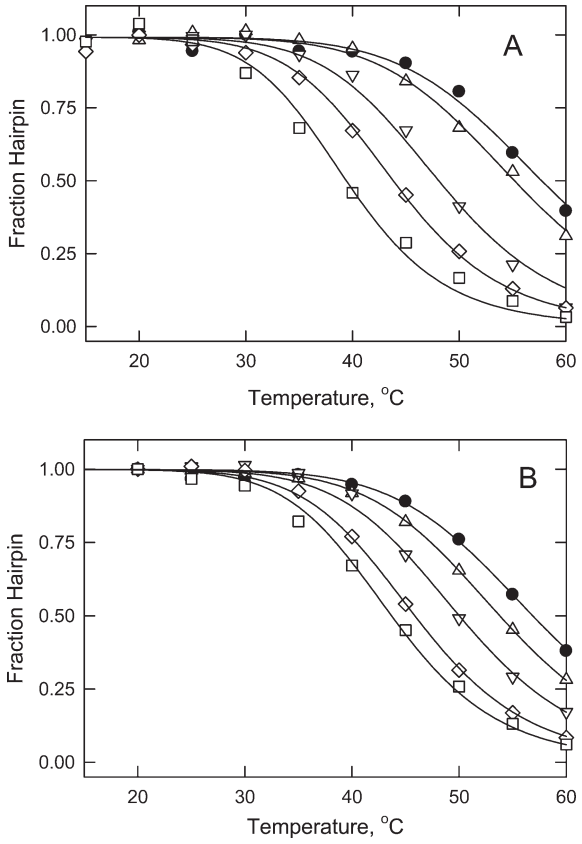

Figure 4. Melting curves observed for the model hairpin in solutions containing organic cations. (A) Dependence of the fractional hairpin concentration on temperature in solutions containing 200 mM: (●) NH_4^+, (△) TMA^+, (▽) TEA^+, (◇) TPA^+, and (□) TBA^+. (B) Dependence of the fractional hairpin concentration on temperature in solutions containing 200 mM: (●) NH_4^+, (△) MPA^+, (▽) DPA^+, (◇) $TriPA^+$, and (□) TPA^+.

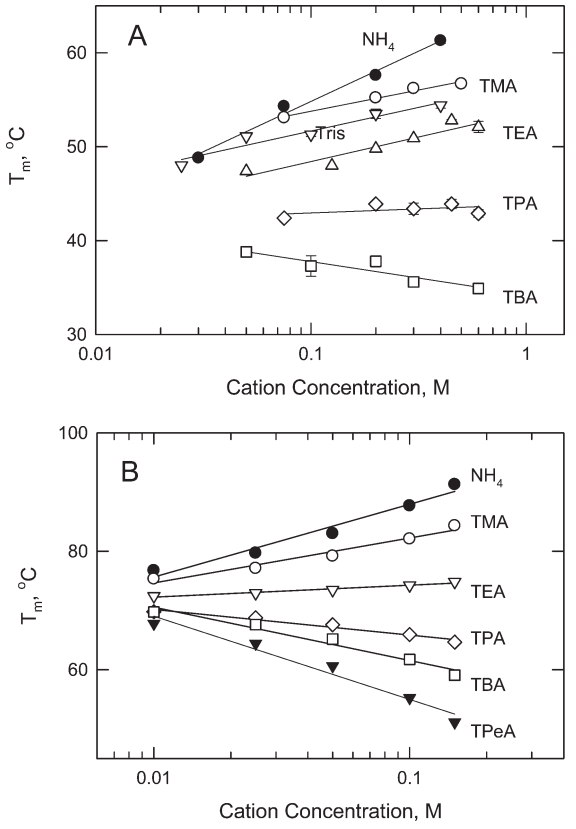

Figure 5. (A) Dependence of the melting temperature, T_m, of the model hairpin on the logarithm of cation concentration in BGEs containing (●) NH_4^+, (▽) $Tris^+$, (○) TMA^+, (△) TEA^+, (◇) TPA^+, and (□) TBA^+. (B) Dependence of the melting temperature of sonicated calf thymus and salmon egg DNAs, determined by UV absorption spectroscopy,[21] on the logarithm of cation concentration in BGEs containing: (●) NH_4^+, (○) TMA^+, (▽) TEA^+, (◇) TPA^+, (□) TBA^+, and (▼) $TPeA^+$. The T_m values were calculated from equations given in ref 21. In both (A) and (B), the lines were drawn by linear regression; the slopes of the lines and correlation coefficients (r^2) are given in Table 1.

containing $Tris^+$, TMA^+, or TEA^+ ions. The nearly zero slope observed in solutions containing TPA^+ suggests that this cation is associated approximately equally well with both the hairpin and coil conformations, so that very few counterions are released upon denaturation. By contrast, the negative slope observed in TBA^+ solutions implies that more TBA^+ ions are associated with the coil conformation than with the hairpin, so that cations are taken up by the coil upon denaturation. For convenience, the slopes of the lines observed for the model hairpin in BGEs containing various cations and the estimated number of cations released (or taken up) per phosphate are tabulated in Table 1.

Similar results have been observed for sonicated calf thymus and salmon egg DNAs,[21] as shown in Figure 5B. The slopes of the lines describing the dependence of the melting temperature on the logarithm of cation concentration increase linearly with cation concentration in solutions containing NH_4^+, TMA^+, and TEA^+ ions and decrease linearly with increasing cation concentration in solutions containing TPA^+, TBA^+, and tetrapentylammonium ($TPeA^+$) ions. The slopes of the lines and the estimated number of cations released (or taken up) per phosphate are summarized in Table 1.

Do the Alkylammonium Ions Act as Denaturants by Site Binding to Random Coils? Collins and Rogers[21] and others[20,23,25] have proposed that large hydrophobic cations act as denaturants by binding to the exposed bases in DNA random coils, driving the helix−coil equilibrium toward the coil conformation. If so, one would expect the melting temperature of the model hairpin, as well

Table 1. Summary of the $dT_m/d(\log [M^+])$ Values Observed for the Model Hairpin and Duplex DNA and the Estimated Number of Cations Released per Phosphate, $\triangle n$

	model hairpin		duplex DNA[a]	
cation	$dT_m/d(\log [M^+])$[b]	$\triangle n$	$dT_m/d(\log [M^+])$[c]	$\triangle n$
Li^+, Na^+, K^+	12.6	0.110	n.d.	
predicted[58,59]	11.4	0.099		
NH_4^+	10.7	0.093	13.4	0.120
$Tris^+$	5.05	0.044	n.d.	
TMA^+	4.52	0.039	8.3	0.072
TEA^+	5.24	0.046	2.2	0.019
TPA^+	0.85	0.007	−4.8	−0.042
TBA^+	−3.51	−0.031	−9.9	−0.086
$TPeA^+$	n.d		−15.4	−0.134

[a] Calculated from equations given in ref 21. [b] The r^2 values ranged from 0.988 to 0.937 for all cations except TPA^+ ($r^2 = 0.232$). [c] $r^2 = 0.960$ for all cations.

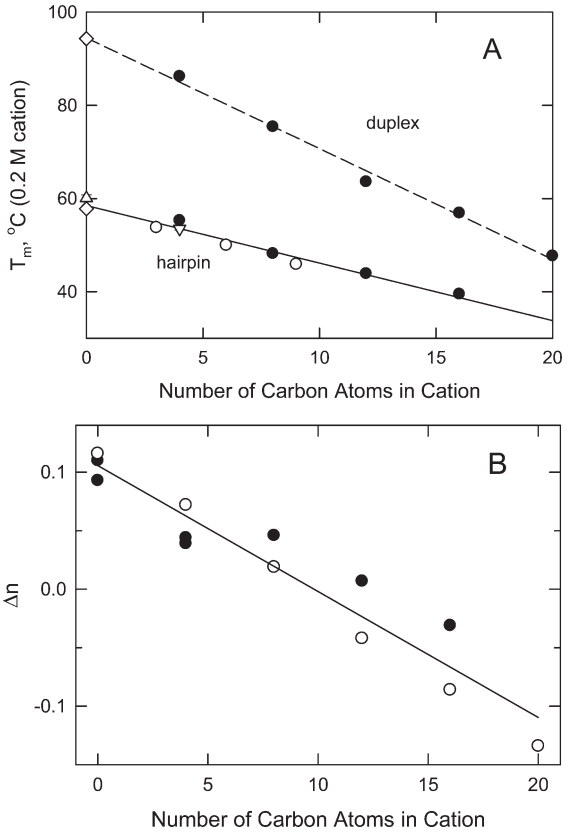

Figure 6. (A) Dependence of the melting temperature, T_m, observed for the model hairpin and duplex DNA[21] on the number of carbon atoms in the cation. All solutions contained 0.2 M cation. The cations are (△) Na^+; (◇) NH_4^+; (▽) $Tris^+$; (○) MPA^+, DPA^+, and $TriPA^+$; and (●) TMA^+, TEA^+, TPA^+, TBA^+, and $TPeA^+$. The T_m values of the duplex were calculated from equations given in ref 21. The lines were drawn by linear regression (r^2 = 0.969 for the model hairpin and 0.998 for the duplex). (B) Dependence of the number of cations released per phosphate on the number of carbon atoms in the cation: (●) model hairpin; (○) duplex DNA.[21] The line was drawn by linear regression (r^2 = 0.920).

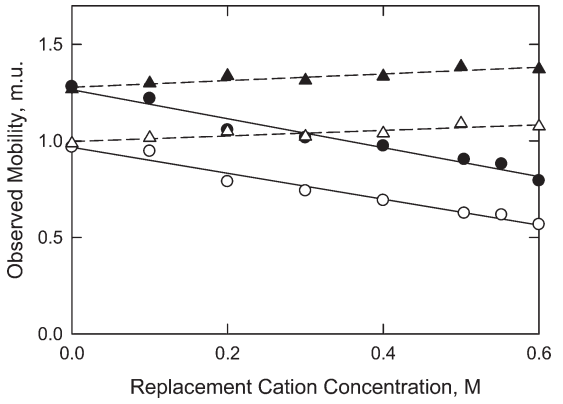

Figure 7. Analysis of cation binding by the replacement ion method. The BGEs in one series of measurements ranged from 0.6 M Na^+ and 0 M NH_4^+ to 0.6 M NH_4^+ and 0 M Na^+ (triangles and dashed lines). In a second experiment, the BGEs ranged from 0.6 M Na^+ and 0 M TBA^+ to 0.6 M TBA^+ and 0 M Na^+ (circles and solid lines). (●, ○) model hairpin; (△, ▲) T16. The lines were drawn by linear regression; the r^2 values are 0.832 and 0.768 for the hairpin and coil, respectively, using NH_4^+ as the replacement ion, and 0.966 and 0.967, respectively, for the hairpin and coil using TBA^+ as the replacement ion.

as duplex DNA, to decrease linearly with the number of carbon atoms in the cation.[21] Figure 6A indicates that the melting temperatures of both the model hairpin and duplex DNA decrease linearly with the number of carbon atoms in the cation. The lines have different slopes, most likely because of the inherently greater thermal stability of high molecular weight duplex DNA. However, despite the differences in size and conformation, similar numbers of cations per phosphate are released (or taken up) upon denaturation of the two DNAs in solutions containing cations with different numbers of carbon atoms, as shown in Figure 6B.

If site binding of the larger tetraalkylammonium ions to the random coil conformation causes DNA denaturation, TBA^+, for example, would be expected to bind to T16 but not to the model hairpin. Conversely, small cations such as NH_4^+, which increase hairpin stability with increasing concentration, might be expected to bind to the model hairpin but not to T16. The possible site binding of NH_4^+ and TBA^+ ions to the model hairpin and T16 was therefore investigated by the replacement ion method.[38] In this method, one cation in the BGE (such as Na^+) is gradually replaced by another cation (such as NH_4^+ or TBA^+), keeping the total cation concentration constant. Plots of the mobility as a function of the concentration of the replacement ion are expected to be linear if preferential cation site binding does not occur or if the two cations bind to the DNA with equal affinities. If preferential cation site binding occurs, the mobility plots will be nonlinear. The results are illustrated in Figure 7. With NH_4^+ as the replacement ion, the mobilities of the model hairpin (closed triangles) and T16 (open triangles) increased linearly with increasing [NH_4^+] (dashed lines), indicating either that no site-specific binding occurs or that the two cations bind equally well to the hairpin and coil conformations. The slopes of the lines are equal within experimental error, as expected because the mobilities observed for the hairpin and T16 in BGEs containing mixed Na^+ and NH_4^+ ions reflect differences in the intrinsic conductivities[70] and viscosity B coefficients[49] of the two ions.[38] The effect of various cations on the hydrogen-bonded structure of water may also play a role in the different mobilities observed in solutions containing different cations.[48,49,71]

With TBA^+ as the replacement ion, the mobilities of the model hairpin (closed circles) and T16 (open circles) decreased linearly with increasing [TBA^+], as indicated by the solid lines in Figure 7. Hence, TBA^+ does not bind in a saturable, site-specific manner to the model hairpin or to DNA random coils. The negative slopes of the lines in BGEs containing TBA^+ ions are greater than the positive slopes observed in BGEs containing NH_4^+ ions because the B coefficient of TBA^+ is significantly greater than the B coefficients of Na^+ or NH_4^+.[49] Hence, the viscosity of the BGE increases significantly with increasing [TBA^+], leading to a corresponding decrease in the observed mobility (see eq 2). The combined results suggest that TBA^+ does not act as a DNA denaturant by site binding to the random coil and pulling the conformational equilibrium toward the coil form. Similar conclusions have been drawn from calorimetric studies of high molecular weight dsDNAs[72] and time-resolved Stokes-shift measurements of small DNA oligomers.[73]

If Not Site Binding, How Do the Alkylammonium Ions Affect DNA Conformational Stability? The various cations used in this study vary not only in hydrophobicity but also in cation size. Therefore, one might expect that the melting temperature observed for the model hairpin in solutions containing a

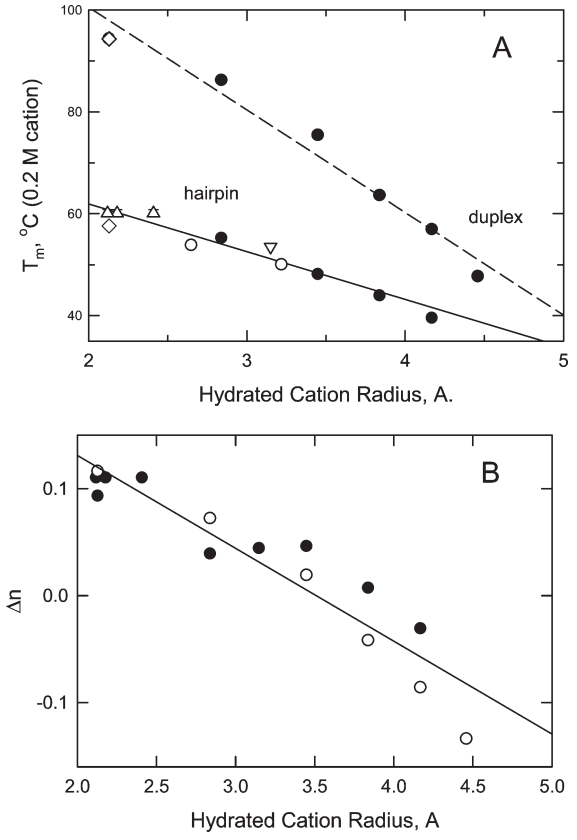

Figure 8. (A) Dependence of the melting temperature of the model hairpin and duplex DNA[21] on the hydrated radius of the cation, in solutions containing 0.2 M cation. The cations are (△) Li^+, Na^+, and K^+; (◇) NH_4^+; (▽) $Tris^+$; (○) MPA^+ and DPA^+; and (●) the tetraalkylammonium ions TMA^+, TEA^+, TPA^+, TBA^+, and $TPeA^+$. The hydrated radii of most of the cations were taken from Marcus;[49,74] the $Tris^+$ radius was taken from ref 75, and the MPA^+ and DPA^+ radii were taken from ref 76. The T_m values of the duplex were calculated from equations given in ref 21. The lines were drawn by linear regression (r^2 = 0.911 for the model hairpin and 0.965 for the duplex). (B) Dependence of the number of cations released per phosphate on cation radius: (●) model hairpin; (○) duplex DNA.[21] The line was drawn by linear regression (r^2 = 0.888).

constant cation concentration would decrease with increasing cation size. As expected, the melting temperature of the model hairpin decreases linearly with the increasing radius of the hydrated cation,[49,74−76] as shown by the solid line in Figure 8A. Similar results are observed for high molecular weight duplex DNAs,[21] as shown by the dashed line in the same figure.

The number of cations released per phosphate is linearly correlated with the radius of the hydrated cation, as shown in Figure 8B. Since the model hairpin and high molecular weight duplex DNAs release approximately the same number of cations per phosphate upon thermal denaturation, the results obtained here for the model hairpin are general and are not restricted to a particular DNA size or secondary structure.

Why Cation Size? Cation size is an important determinant of DNA conformational stability because larger cations cannot physically approach the DNA backbone as closely or as densely as smaller cations. In addition, the decreased surface charge density of the larger cations would decrease the strength of the Coulombic interactions between the cations and the phosphate residues. Not surprisingly, recent atomic emission spectroscopy measurements have shown that number of cations located in the immediate vicinity of the DNA duplex correlates inversely with cation size.[69]

Adjacent phosphate residues in B-form DNA are separated by 3.3 Å in the vertical direction and 5 Å in the horizontal direction.[77] It is not a coincidence that cations with a hydrated radius of 3.3 Å or less (Li^+, Na^+, K^+, NH_4^+, TMA^+, $Tris^+$, and TEA^+)[49,74,75] are preferentially condensed onto and/or closely associated with the hairpin stem and with duplex DNA by interacting electrostatically with the closely spaced phosphate residues in the native conformation. Upon thermal denaturation, some of these cations are released because of the lower charge density of the random coil, where the phosphate residues are separated by 3.4−6.3 Å, depending on the method used to measure the separation.[12,13,29,60]

TPA^+, with a hydrated radius of 3.84 Å,[49,74] appears to interact equally well with the hairpin and coil conformations because the melting temperature is nearly independent of [TPA^+] (Figure 5A). TBA^+, with a hydrated radius of 4.17 Å,[49,74] appears to be preferentially associated with the random coil conformation because the melting temperatures of both the model hairpin and duplex DNA decreased with increasing [TBA^+]. TBA^+ ions therefore preferentially stabilize the coil conformation, at least in part because they can more effectively shield the negative charges of the widely spaced phosphate residues. Mutual hydrophobic interactions between TBA^+ ions condensed on the surface of DNA random coils may also stabilize the coil conformation, since previous studies have shown that TBA^+ ions can self-associate and form chains linking negatively charged micelles together.[78]

SUMMARY AND CONCLUDING REMARKS

The studies described here have compared the effect of various monovalent cations on the thermal stability of a small DNA hairpin. At constant cation concentration, the melting temperature of the model hairpin decreases in the order $Li^+ \sim Na^+ \sim K^+ > NH_4^+ > TMA^+ > Tris^+ > TEA^+ > TPA^+ > TBA^+$. The progressive decrease in the melting temperature with increasing cation hydrophobicity is not due to site-binding of the more hydrophobic cations to DNA random coils, pulling the helix−coil equilibrium toward the coil conformation, because no evidence was found for preferential cation binding either to the model hairpin or the random coil oligomer, T16.

Instead, cation size appears to be an important determinant of DNA conformational stability. Cation size is important because the larger cations cannot physically approach the phosphate residues in B-form DNA as closely as smaller cations, weakening the Coulombic interactions with the phosphate groups and decreasing the effectiveness of electrostatic shielding.[69,79] By contrast, electrostatic shielding of the phosphate residues in the random coil conformation would be more effective for the larger cations, which can more easily span the distance between adjacent phosphate residues in flexible, single-stranded DNAs. When the electrostatic shielding effects are in balance, so that the hairpin and coil conformations are equally stabilized by a given cation, the melting temperature is essentially independent of cation concentration, as observed for the model hairpin in solutions containing TPA^+ ions.

Hydrophobic effects appear to play a less direct role in DNA stabilization than cation size. TMA^+, which increases the melting temperature of B-form DNA with increasing concentration, could enter the grooves and interact with the nucleotide bases

as well as the phosphate groups. However, small-angle neutron scattering measurements have shown that TMA^+ does not significantly penetrate the grooves of duplex DNA,[80] suggesting that the electrostatic shielding effects of this cation are more important than hydrophobic interactions.

TPA^+ has little or no effect on the stability of the model hairpin, suggesting that TPA^+ interacts equally well with both the helix and coil conformations. If hydrophobic effects were dominant, TPA^+ would be expected to decrease the stability of the model hairpin, as it does for duplex DNA.[21] The difference between the results observed for the model hairpin and duplex DNA may be due to end effects that decrease the number of cations condensed around small DNAs.[81,82]

Larger hydrophobic cations, such as TBA^+, preferentially stabilize the coil conformation with increasing concentration, in part because of the relatively more effective electrostatic shielding of the phosphate residues in the coil. Mutual interactions between TBA^+ ions condensed on the surface of the coil, if they occur, would amplify the affinity of large hydrophobic cations for the coil conformation. In addition, cation size and hydrophobicity could affect DNA thermal stability by through-solvent effects on the hydrogen-bonded structure of water.[83−86] Nonlinear Poisson−Boltzmann calculations of the effect of cation size on the thermal stability of DNA hairpins and duplexes would be interesting but are beyond the scope of the present study.

AUTHOR INFORMATION

Corresponding Author

*Tel: (319) 335-7896. Fax: (319) 335-9570. E-mail: nancy-stellwagen@uiowa.edu.

Present Address

[†]410 Harvard Lane, Bartlett, IL 60103.

Funding Sources

This work was supported in part by Grant CHE0748271 from the Analytical and Surface Chemistry Program of the National Science Foundation (to N.C.S.).

ABBREVIATIONS

BGE, background electrolyte; CE, capillary electrophoresis; DM, diethylmalonate; EOF, electroosmotic flow; m.u., mobility unit ($1\ \text{m.u.} = 1 \times 10^{-4}\ \text{cm}^2/(\text{V s})$); TMA^+, tetramethylammonium ion; TEA^+, tetraethylammonium ion; TPA^+, tetrapropylammonium ion; TBA^+, tetrabutylammonium ion; $TPeA^+$, tetrapentylammonium ion.

REFERENCES

(1) Hamaguchi, K., and Geiduschek, E. P. (1962) The effect of electrolytes on the stability of the deoxyribonucleate helix. *J. Am. Chem. Soc. 84*, 1329–1338.

(2) Schildkraut, C., and Lifson, S. (1965) Dependence of the melting temperature of DNA on salt concentration. *Biopolymers 3*, 195–208.

(3) Gruenwedel, D. W., and Hsu, C.-H. (1969) Salt effects on the denaturation of DNA. *Biopolymers 7*, 557–570.

(4) Gruenwedel, D. W., Hsu, C.-H., and Lu, D. S. (1971) The effects of aqueous neutral-salt solutions on the melting temperatures of deoxyribonucleic acids. *Biopolymers 10*, 47–68.

(5) Elson, E. L., Scheffler, I. E., and Baldwin, R. L. (1970) Helix formation by d(TA) oligomers. III. Electrostatic effects. *J. Mol. Biol. 54*, 401–415.

(6) Pegram, L. M., Wendorff, T., Erdmann, R., Shkel, I., Bellissimo, D., Felitsky, D. J., and Record, M. T., Jr. (2010) Why Hofmeister effects of many salts favor protein folding but not DNA helix formation. *Proc. Natl. Acad. Sci. U.S.A. 107*, 7716–7721.

(7) Haasnoot, C. A. G., de Bruin, S. H., Hilbers, C. W., van der Marel, G. A., and van Boom, J. H. (1985) Loop structures in synthetic oligonucleotides. Hairpin stability and structure studied as a function of loop elongation. *Proc. Int. Symp. Biomol. Struct. Interact. Suppl. J. Biosci. 8*, 767–780.

(8) Record, M. T., Jr. (1975) Effects of Na^+ and Mg^{+2} ions on the helix-coil transition of DNA. *Biopolymers 14*, 2137–2158.

(9) Draper, D. E. (2004) A guide to ions and RNA structure. *RNA 10*, 335–343.

(10) Draper, D. E. (2008) RNA folding: thermodynamic and molecular descriptions of the roles of ions. *Biophys. J. 95*, 5489–5495.

(11) Bai., Y., Das, R., Millett, I. S., Herschlag, D., and Doniach, S. (2005) Probing counterion modulated repulsion and attraction between nucleic acid duplexes in solution. *Proc. Natl. Acad. Sci. U.S.A. 102*, 1035–1040.

(12) Manning, G. (1978) The molecular theory of polyelectrolyte solutions with applications to the electrostatic properties of polynucleotides. *Q. Rev. Biophys. 11*, 179–246.

(13) Record, M. T., Jr., Anderson, C. F., and Lohman, T. M. (1978) Thermodynamic analysis of ion effects on the binding and conformational equilibria of proteins and nucleic acids: the roles of ion association or release, screening, and ion effects on water activity. *Q. Rev. Biophys. 11*, 103–178.

(14) Record, M. T., Jr., Zhang, W., and Anderson, C. F. (1998) Analysis of effects of salts and uncharged solutes on protein and nucleic acid equilibria and processes: a practical guide to recognizing and interpreting polyelectrolyte effects, Hofmeister effects, and osmotic effects of salts. *Adv. Protein Chem. 51*, 281–353.

(15) Dix, D. E., and Straus, D. B. (1972) DNA helix stability. I. Differential stabilization by counter cations. *Arch. Biochem. Biophys. 1552*, 299–310.

(16) Scott, J. N., Nucci, N. V., and Vanderkooi, J. M. (2008) Changes in water structure induced by the guanidinium cation and implications for protein denaturation. *J. Phys. Chem. A 112*, 10939–10948.

(17) von Hippel, P. H., and Wong, K.-Y. (1964) Neutral salts: the generality of their effects on the stability of macromolecular conformations. *Science 145*, 577–580.

(18) von Hippel, P. H., and Schleich, T. (1969) Ion effects on the solution structure of biological macromolecules. *Acc. Chem. Res. 2*, 257–265.

(19) Robinson, D. R., and Grant, M. E. (1966) The effects of aqueous salt solutions on the activity coefficients of purine and pyrimidine bases and their relation to the denaturation of deoxyribonucleic acid by salts. *J. Biol. Chem. 241*, 4030–4042.

(20) Melchior, W. B., Jr., and von Hippel, P. H. (1973) Alteration of the relative stability of dA·dT and dG·dC base pairs in DNA. *Proc. Natl. Acad. Sci. U.S.A. 70*, 298–302.

(21) Collins, J. M., and Rogers, K. S. (1977) Melting point depression of DNA by tetraalkylammonium bromides. *Chem.-Biol. Interact. 19*, 197–203.

(22) Orosz, J. M., and Wetmur, J. G. (1977) DNA melting temperatures and renaturation rates in concentrated alkylammonium salt solutions. *Biopolymers 16*, 1183–1199.

(23) Trend, B. L., Knoll, D. A., Ueno, M., Evans, D. F., and Bloomfield, V. A. (1990) Cation radius effects on the helix-coil transition of DNA. *Biophys. J. 57*, 829–834.

(24) Rees, W. A., Yager, T. D., Korte, J., and von Hippel, P. H. (1993) Betaine can eliminate the base pair composition dependence of DNA melting. *Biochemistry 32*, 137–144.

(25) Strauss, U. P., Helfgott, C., and Pink, H. (1967) Interactions of polyelectrolytes with simple electrolytes. II. Donnan equilibria obtained with DNA in solutions of 1−1 electrolytes. *J. Phys. Chem. 71*, 2550–2556.

(26) Blommers, M. J. J., Walters, J. A. L. I., Haasnoot, C. A. G., Aelen, J. M. A., van der Marel, G. A., van Boom, J. H., and Hilbers, C. W. (1989)

Effects of base sequence on the loop folding in DNA hairpins. *Biochemistry 28*, 7491–7498.

(27) Haasnoot, C. A. G., de Bruin, S. H., Berendsen, R. G., Janssen, H. G. J. M., Binnendijk, T. J. J., Hilbers, C. W., van der Marel, G. A., and van Boom, J. H. (1983) Structure, kinetics and thermodynamics of DNA hairpin fragments in solution. *J. Biomol. Struct. Dyn. 1*, 115–129.

(28) Camerman, N., Fawcett, J. K., and Camerman, A. (1976) Molecular structure of a deoxyribose-dinucleotide, sodium thymidylyl-(5′→3′)-thymidylate-(5′) hydrate (pTpT), and a possible structural model for polythymidylate. *J. Mol. Biol. 107*, 601–621.

(29) Murphy, M. C., Rasmik, I., Cheng, W., Lohman, T. M., and Ha, T. (2004) Probing single-stranded DNA conformational flexibility using fluorescence spectroscopy. *Biophys. J. 86*, 2530–2537.

(30) Saenger, W. (1983) *Principles of Nucleic Acid Structure*, Springer-Verlag, New York.

(31) Doose, S., Barsch, H., and Sauer, M. (2007) Polymer properties of polythymine as revealed by translational diffusion. *Biophys. J. 93*, 1224–1234.

(32) Stellwagen, E., Abdulla, A., Dong, Q., and Stellwagen, N. C. (2007) Electrophoretic mobility is a reporter of hairpin structure in single-stranded DNA oligomers. *Biochemistry 46*, 10931–10941.

(33) Stellwagen, E., Renze, A., and Stellwagen, N. C. (2007) Capillary electrophoresis is a sensitive monitor of the hairpin-random coil transition in DNA oligomers. *Anal. Biochem. 365*, 103–110.

(34) Zeng, Y., and Zocchi, G. (2006) Mismatches and bubbles in DNA. *Biophys. J. 90*, 4522–4529.

(35) Stellwagen, N. C., Gelfi, C., and Righetti, P. G. (1997) The free solution mobility of DNA. *Biopolymers 42*, 687–703.

(36) Stellwagen, E., and Stellwagen, N. C. (2003) Probing the electrostatic shielding of DNA with capillary electrophoresis. *Biophys. J. 84*, 1855–1866.

(37) Stellwagen, N. C., and Stellwagen, E. (2009) Effect of the matrix on DNA electrophoretic mobility. *J. Chromatogr. A 1216*, 1917–1929.

(38) Stellwagen, E., Dong, Q., and Stellwagen, N. C. (2007) Quantitative analysis of monovalent counterion binding to random-sequence, double-stranded DNA using the Replacement Ion method. *Biochemistry 46*, 2050–2058.

(39) Viovy, J.-L. (2000) Electrophoresis of DNA and other polyelectrolytes: physical mechanisms. *Rev. Mod. Phys. 72*, 813–872.

(40) Manning, G. S. (1981) Limiting laws and counterion concentration in polyelectrolyte solutions. 7. Electrophoretic mobility and conductance. *J. Phys. Chem. 85*, 1506–1515.

(41) Pitts, W., Tabor, B. E., and Daly, J. (1970) Concentration dependence of electrolyte conductance. 2. Comparison of experimental data with the Fuoss-Onsager and Pitts treatments. *Trans. Faraday Soc. 66*, 693–707.

(42) O'Brien, R. W., and White, L. R. (1978) Electrophoretic mobility of a spherical colloidal particle. *J. Chem. Soc., Faraday Trans. 74*, 1607–1626.

(43) Cleland, R. L. (1991) Electrophoretic mobility of wormlike chains: II. Theory. *Macromolecules 24*, 4391–4402.

(44) Honig, B., and Nicholls, A. (1995) Classical electrostatics in biology and chemistry. *Science 268*, 1144–1149.

(45) Boström, M., Kunz, W., and Ninham, B. W. (2005) Hofmeister effects in surface tension of aqueous electrolyte solution. *Langmuir 21*, 2619–2623.

(46) Ball, P. (2008) Water as an active constituent in cell biology. *Chem. Rev. 108*, 74–108.

(47) Zhang, Y., and Cremer, P. S. (2009) The inverse and direct Hofmeister series for lysozyme. *Proc. Natl. Acad. Sci. U.S.A. 106*, 15249–15253.

(48) Arakawa, T., and Timasheff, S. N. (1982) Preferential interactions of proteins with salts in concentrated solutions. *Biochemistry 21*, 6545–6552.

(49) Marcus, Y. (1997) *Ion Properties*, Marcel Dekker, New York.

(50) Marky, L. A., and Breslauer, K. J. (1987) Calculating thermodynamic data for transitions of any molecularity from equilibrium melting curves. *Biopolymers 26*, 1601–1620.

(51) Xodo, L. E., Manzini, G., Quadrifoglio, F., van der Marel, G. A., and van Boom, J. H. (1986) Thermodynamic behaviour of the heptadacadeoxynucleotide d(CGCGCGTTTTTCGCGCG). *Nucleic Acids Res. 14*, 5389–5397.

(52) Mandell, K. E., Vallone, P. M., Owczarzy, R., Riccelli, P. T., and Benight, A. S. (2006) Studies of DNA dumbbells. VIII. Melting analysis of DNA dumbbells with dinucleotide repeat stem sequences. *Biopolymers 82*, 199–221.

(53) Rentzeperis, D., Kharakoz, D. P., and Marky, L. A. (1991) Coupling of sequential transitions in a DNA double hairpin: energetics, ion binding, and hydration. *Biochemistry 30*, 6276–6283.

(54) Rentzeperis, D., Alessi, K., and Marky, L. A. (1993) Thermodynamics of DNA hairpins: contribution of loop size to hairpin stability and ethidium binding. *Nucleic Acids Res. 21*, 2683–2689.

(55) Peyret, N. (2000) Prediction of nucleic acid hybridization: parameters and algorithms. Ph.D. Dissertation, Wayne State University, Department of Chemistry, Detroit, MI.

(56) SantaLucia, J., Jr. (1998) A unified view of polymer, dumbbell, and oligonucleotide DNA nearest-neighbor thermodynamics. *Proc. Natl. Acad. Sci. U.S.A. 95*, 1460–1465.

(57) SantaLucia, J., Jr., and Hicks, D. (2004) The thermodynamics of DNA structural motifs. *Annu. Rev. Biophys. Biomol. Struct. 33*, 415–440.

(58) Zuker, M. (2003) Mfold web server for nucleic acid folding and hybridization prediction. *Nucleic Acids Res. 31*, 3406–3415.

(59) Markham, N. R., and Zuker, M. (2005) DINAMelt web server for nucleic acid melting prediction. *Nucleic Acids Res. 33*, W577–W581.

(60) Bond, J. P., Anderson, C. F., and Record, M. T., Jr. (1994) Conformational transitions of duplex and triplex nucleic acid helices: thermodynamic analysis of effects of salt concentration on stability using preferential interaction coefficients. *Biophys. J. 67*, 825–836.

(61) Shkel, I. A., and Record, M. T., Jr. (2004) Effect of the number of nucleic acid oligomer charges on the salt dependence of stability (ΔG^{o}_{37}) and melting temperature (T_m): NLPB analysis of experimental data. *Biochemistry 43*, 7090–7101.

(62) Chu, V. B., Bai, Y., Lipfert, J., Herschlag, D., and Doniach, S. (2008) A repulsive field: advances in the electrostatics of the ion atmosphere. *Curr. Opin. Chem. Biol. 12*, 619–625.

(63) Tan, Z.-J., and Chen, S.-J. (2005) Electrostatic correlations and fluctuations for ion binding to a finite length polyelectrolyte. *J. Chem. Phys. 122*, 044903.

(64) Tan, Z.-J., and Chen, S.-J. (2005) Nucleic acid helix stability: effects of salt concentration, cation valence and size, and chain length. *Biophys. J. 90*, 1175–1190.

(65) Tan, Z.-J., and Chen, S.-J. (2008) Salt dependence of nucleic acid hairpin stability. *Biophys. J. 95*, 738–752.

(66) Tan, Z.-J., and Chen, S.-J. (2010) Predicting ion binding properties for RNA tertiary structures. *Biophys. J. 99*, 1565–1576.

(67) Draper, K. E. (2008) RNA folding: thermodynamic and molecular descriptions of the roles of ions. *Biophys. J. 95*, 5489–5495.

(68) Lambert, D., Leipply, D., Shiman, R., and Draper, D. E. (2009) The influence of monovalent cation size on the stability of RNA tertiary structures. *J. Mol. Biol. 390*, 791–804.

(69) Bai, Y., Greenfeld, M., Travers, K. J., Chu, V. B., Lipfert, J., Doniach, S., and Herschlag, D. (2007) Quantitative and comprehensive decomposition of the ion atmosphere around nucleic acids. *J. Am. Chem. Soc. 129*, 14981–14988.

(70) Weast, R. C., Ed. (1984) *CRC Handbook of Chemistry and Physics*, 65th ed., pp D171−D172, CRC Press, Boca Raton, FL.

(71) Stellwagen, E., Dong, Q., and Stellwagen, N. C. (2005) Monovalent cations affect the free solution mobility of DNA by perturbing the hydrogen-bonded structure of water. *Biopolymers 78*, 62–68.

(72) Matulis, D., Rouzina, I., and Bloomfield, V. A. (2002) Thermodynamics of cationic lipid binding to DNA and DNA condensation: roles of electrostatics and hydrophobicity. *J. Am. Chem. Soc. 124*, 7331–7342.

(73) Sen, S., Gearheart, L. A., Rivers, E., Liu, H., Coleman, R. S., Murphy, C. J., and Berg, M. A. (2006) Role of monovalent counterions in the ultrafast dynamics of DNA. *J. Phys. Chem. B 110*, 13248–13255.

(74) Marcus, Y. (1994) A simple empirical model describing the thermodynamics of hydration of ions of widely varying charges, sizes, and shapes. *Biophys. Chem. 51*, 111–127.

(75) Rudman, R., Eilerman, D., and La Placa, S. J. (1978) The structure of crystalline Tris: a plastic crystal precursor, buffer, and acetylcholine attenuator. *Science 200*, 531–533.

(76) Aue, D. H., Webb, H. M., and Bowers, M. T. (1976) A thermodynamic analysis of solvation effects on the basicities of alkylamines. An electrostatic analysis of substituent effects. *J. Am. Chem. Soc. 98*, 318–329.

(77) Calladine, C. R., Drew, H. R. (1992) *Understanding DNA*, p 26, Academic Press, London.

(78) Zana, R., Benrraou, M., and Bales, B. L. (2004) Effect of the nature of the counterion on the properties of anionic surfactants. 3. Self-association behavior of tetrabutylammonium dodecyl sulfate and tetradecylsulfate: clouding and micellar growth. *J. Phys. Chem. B 108*, 18195–18203.

(79) Bai, Y., Chu, V. B., Lipfert, J., Pande, V. S., Herschlag, D., and Doniach, S. (2008) Critical assessment of nucleic acid electrostatics via experimental and computational investigation of an unfolded state ensemble. *J. Am. Chem. Soc. 130*, 12334–12341.

(80) Dai, L., Mu, Y., Nordenskiöld, Lapp, A., and van der Maarel, J. R. C. (2006) Charge structure and counterion distribution in hexagonal DNA liquid crystal. *Biophys. J. 92*, 947–958.

(81) Fenley, M. O., Manning, G. S., and Olson, W. K. (1990) Approach to the limit of counterion condensation. *Biopolymers 30*, 1191–1203.

(82) Stein, V. M., Bond, J. P., Capp, M. W., Anderson, C. F., and Record, M T., Jr. (1995) Importance of coulombic end effects on cation accumulation near oligoelectrolyte B-DNA: a demonstration using ^{23}Na NMR. *Biophys. J. 68*, 1063–1072.

(83) Tamaki, K. (1974) The surface activity of tetra-n-alkylammonium halides in aqueous solutions. The effect of hydrophobic hydration. *Bull. Chem. Soc. Jpn. 47*, 2764–2767.

(84) Pittz, E. P., and Timasheff, S. N. (1978) Interaction of ribonuclease A with aqueous 2-methyl-2.4-pentanediol at pH 5.8. *Biochemistry 17*, 615–623.

(85) Arakawa, T., and Timasheff, S. N. (1982) Preferential interactions of proteins with salts in concentrated solutions. *Biochemistry 21*, 6545–6552.

(86) Hultgren, A., and Rau, D. C. (2004) Exclusion of alcohols from spermidine-DNA assemblies: probing the physical basis of preferential hydration. *Biochemistry 43*, 8272–8280.